Comparing models of the structure factor for warm dense matter

Contact d.riley@qub.ac.uk

D. Riley, F. Y. Khattak, J. J. Angulo Gareta, E. García Saiz, G. Shabbir Naz, J. Kohanoff, S. Sahoo, S. F. C. Shearer and K. A. Thornton
School of Mathematics and Physics, Queens University Belfast, University Road, Belfast BT7 1NN, UK

C. Gregory and N. C. Woolsey
University of York, Heslington, York Y010 5DD, UK

M. Notley and D. Neely
Central Laser Facility, STFC, Rutherford Appleton Laboratory, HSIC, Didcot, Oxon OX11 0QX, UK

Introduction

Warm dense matter (WDM) is a state intermediate between the solid state, where Coulomb forces dominate over thermal motion and classical plasmas where the converse is the case. Its physical characteristics include partial electron degeneracy with $T \sim T_F$ where T_F is the Fermi temperature, and strong ion-ion coupling.

Such matter is of importance, primarily due to its relevance to planetary interiors [1] and inertial fusion experiments. One method for diagnosing such matter is by X-ray scattering [2-4]. For a quasi-monochromatic X-ray scatter source we can expect a spectrally integrated scatter signal, $I(q)$, of the form below [5,6];

$$I(q) = I_T \left[(f_i(q) + \rho(q))^2 S_{ii}(q) + Z_b S^{inc}(q) + Z_f S_{ee}(q) \right]$$

where q is the scatter momentum I_T is the classical Thomson cross-section for an electron, f_i is the ionic form factor, $\rho(q)$ is the electron-ion correlation term and $S_{ii}(q)$ is the static ion-ion structure factor. These terms come together to give us the quasi-coherent Rayleigh scatter from the ions. The terms $S^{inc}(q)$ and $S_{ee}(q)$ refer, respectively, to the incoherent bound-free Compton scatter from Z_b bound electrons and the static electron structure factor for scatter from Z_f free electrons per atom. For a moderate Z plasma at modest temperature, the latter two terms can be small compared to the Rayleigh scatter e.g. for Al at conditions in the current experiment, we expect ~10 bound electrons compared to 3 free.

Since the ion structure factor scales as Z^2, we can see how Rayleigh scatter dominates. Indeed, in an earlier paper [7] it was seen in high resolution scatter spectra that the Rayleigh scatter was clearly dominant over incoherent (spectrally shifted) scatter.

Experimental setup

The experiment was performed in TAE of Vulcan. The main six beams, delivering nominally 600 ps pulses of ~100 J in second harmonic were focused in two opposing groups of 3 onto the sample (see figure 1). We used 3 mm phased zone plates (PZP) combined with f/10 lens to make a smooth flat top focal spot. The pulse shape in second harmonic was measured with the use of an optical streak camera. The peak intensity achieved on target was ~5×10^{12} Wcm^{-2}.

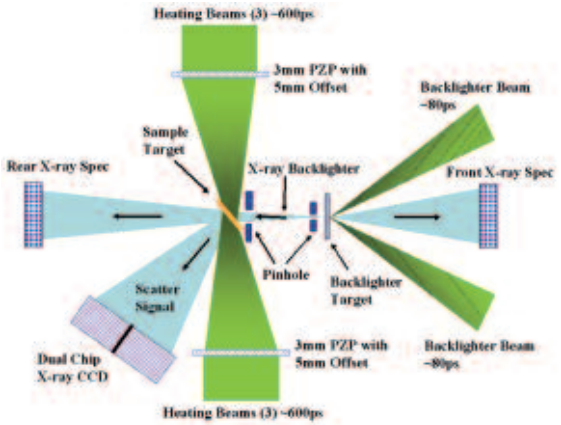

Figure 1. Schematic of experiment.

The target sample was a sandwich consisting of 4.5/6/4.5 μm of CH/Al/CH. The Al scatters by far more due to the much higher number of bound electrons per atoms, especially when the CH layer has been heated by the shock driving beams.

A HYADES [8] simulation of the density and temperature for 3 different times after the start of the pulse reaching the target surface can be seen in figure 2. The graphs show only the conditions for the Al core of the sample. The simulation used multi-group radiation transfer with 35 groups logarithmically spaced from 0.01-15 keV and the SESAME equation of state tables [9]. In an earlier publication [7] we showed that for one sided irradiation of similar targets at similar pulse durations and intensities, the time for shock breakout predicted by HYADES closely matched experimental measurements.

Two beams of 80 ps duration were also frequency doubled and synchronously focused with f/5 lens onto a 3 micron thick Ti target to generate the backlighting X-ray beam. The intensity on target was controlled by changing the focal spot dimension. The back-lighter X-ray signal principally consisted of the He-α line ($1s^2$-$1s2p\ ^1P$ and satellites) emission at 4.7-4.75 keV. This is the dominant spectral feature in the few keV spectral region and the signal had a duration similar to the optical pulse [10] thus allowing ~100 ps resolution. The emission level was monitored with the help of two flat-crystal spectrometers coupled CCD systems, one in

the rear employing Si (111) and one in the front of the target making use of Ge (220) crystal. After passing through an array of two pinholes, the probing X-ray back-lighter beam was restricted to a narrow cone which determines the angular resolution of the experiment. This narrow cone was then incident on the sample. However, high resolution restricts the incident signal to a lower signal level and a spread of 4° was employed as a compromise between resolution and signal level. This meant that the X-ray probe covered a focal spot ~1×1.4 mm, somewhat smaller than the shocked area. By delaying the back-lighter beams relative to the shock driving beams, the back-lighter X-ray beam interacted at different time delay with the plasma generated by main beams. The Andor dual-chip X-ray CCD system, covering a range of 50° to 80° scattered angle, was used to count individual scatter photons, with each photon creating ~130 counts. Appropriate shielding was in place to block X-rays from the back-lighter source hitting the CCD directly. As for previous experiments, in order to ensure that we have only scattering from the shock compressed region, we took several test shots where the entire assembly including the target holder was put into place but without the actual sample foil- the subsequent shots resulted in detected photon counts less than 5% of the typical scatter signals, thus demonstrating that our signals come from the shocked sample.

The dual chip CCD has two chips sited side by side. The chips were ~12 cm from the sample. Each third of a chip subtended ~4.5° thus matching the angular resolution of the probe cone of X-rays. We made histograms centered about five positions on each chip so as to "over-sample". Filtering of 250 μm Be, 72 μm Mylar and 39 μm Al allowed transmission of just under 6% of the Ti-He-α photons whilst severely suppressing the keV photon emission from the hot CH plasma on

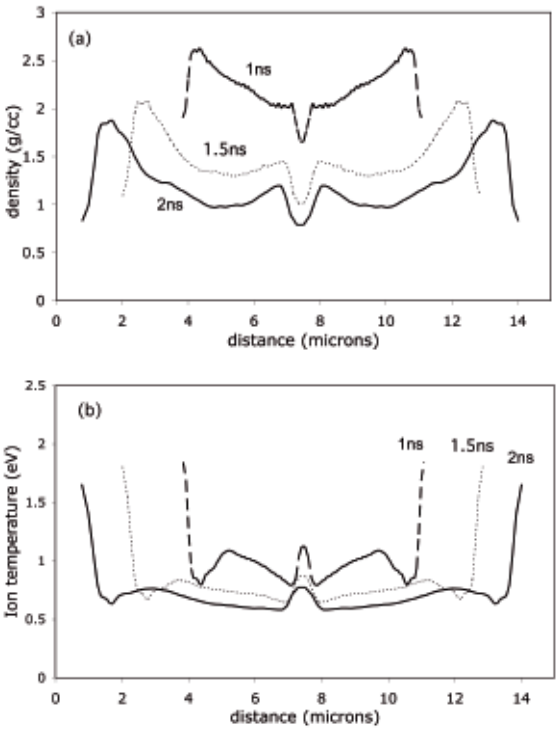

Figure 2. Hyades simulation of the Al foil in the sandwich targets.

the surface of the samples. As in earlier, work,[11] we use single photon counting to measure the number of photons scattered into each unit of solid angle. Although the crystal spectrometers monitoring the throughput of the back-lighter source onto the target gave us shot to shot comparisons, the crystals were not absolutely calibrated and so comparisons with theory in this paper are made with respect to variation with angle rather than absolute cross-sections.

Results

In figure 3, we see cross-section measurements taken at 1.5 ns and at 2 ns after the start of the shock driving beams. The error bars are based on counting statistics of the photons in each histogram. We have compared the data to some simulations. Firstly, we can see that the one component plasma (OCP) model predicts a distinctive peak. However, a molecular dynamics model based on an embedded atom potential fits the shape of the experimental data very well. We have used this type of model[12,13] previously[7] and it effectively accounts for multi-body interactions and screening, whereas the OCP model does not include screening effects at all. We can readily understand why the unscreened OCP does not work by considering the screening length, λ expected (eg see[14]):

$$\lambda^{-2} = \frac{4e^2 m_e}{\pi \hbar^3} \int f_e(p) dp$$

where we have used the Fermi-Dirac distribution for electrons with momentum, p. By using this, we can calculate that for our conditions the screening length is only about a third of the inter-ion radius, R_i. This

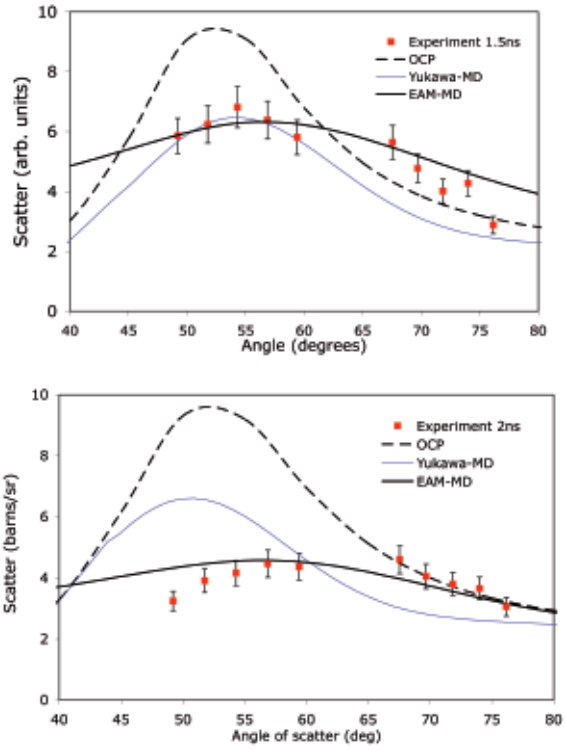

Figure 3. Experimental data compared to simulations. The absolute experimental cross-sections are uncertain due to lack of absolute calibration but have been scaled to show the fit to the EAM model. Simple scaling alone cannot give a good fit to the other models.

means that instead of having a strong coupling parameter varying from $\Gamma=Z^*e^2/kT_iR_i$ ~60-80, we have an effective range of Γ ~ 2-3. This means that we do not expect the OCP model to work. With this in mind, we have also compared the data to a screened Coulombic potential of form:

$$V(r) = \frac{Ze^2}{4\pi\epsilon_0 r} e^{-r/\lambda}$$

with λ determined as above. We can see that, although the effects of screening are obvious from comparison with the OCP, the fit to the data is still not as good as for the EAM-MD simulation.

Conclusions

We have made angularly resolved X-ray scatter measurements from a warm dense matter sample. The electron density is not high enough to allow screening by electrons to be neglected. By using an embedded atom model we have fitted the shape of the data well, although we do not have absolute calibration. A comparison with an unscreened simulation shows the degree to which screening makes a difference. Interestingly, a model using a linear screening model (Yukawa potential) did not match the data as well as the embedded atom approach.

The significance of this work is that we have moved from the demonstration of scattering and the demonstration of the importance of screening[7] into a new phase where we can think of comparing screening models.

Acknowledgements

The experiment and simulation work was funded by EPSRC under grants GR/R09572/01 and EP/D031532/1. G Shabbir Naz was funded by the Higher Education Council of Pakistan.

References

1. S. Ichimaru, *Reviews of Modern Physics* **54**, 1017 (1982).
2. N. C. Woolsey, D. Riley, E. Nardi, *Rev. Sci. Inst.* **69**, 418 (1998).
3. D. Riley *et al.*, *Phys. Rev. Lett*. **84**, 1704 (2000).
4. S. H. Glenzer *et al.*, *Phys. Rev. Lett*. **90**, 175002 (2003).
5. J. Chihara, *J. Phys.: Condens. Matter* **2**, 231 (2000).
6. E. Nardi, *Phys. Rev. A* **43**, 1977 (1991).
7. E. Garcia Saiz, *Phys. Rev. Lett*. **101**, 075003 (2008).
8. J. T. Larsen and S. M. Lane, *J. Quant. Spectrosc. Radiat. Transfer* **51**, 179 (1994).
9. S. P. Lyon and J. D. Johnson, Group T-1, Los Alamos National Laboratory Technical Report LA-UR-92E3407 (1992).
10. D. Riley, N. C. Woolsey, D. McSherry, F. Y. Khattak and I. Weaver, *Plasma Sources Sci. Technol*. **11**, 484 (2002).
11. D. Riley, N. C. Woolsey, D. McSherry and E. Nardi, *J. Quant. Spectrosc. Radiat. Transfer*, **65**, 463 (2000).
12. M. S. Daw and M. I. Baskes, *Phys. Rev. B*, **29**, 6443 (1984).
13. J. Mei and J. W. Davenport, *Phys. Rev. B*, **46**, 21 (1992).
14. K. Wünsch, J. Vorberger and D. O. Gericke, *Phys. Rev. E*, **79**, 010201 R (2009).